Citation: Molecular Therapy–Nucleic Acids (2013) 2, e89; doi:10.1038/mtna.2013.8

www.nature.com/mtna

Inhibition of *Sox2* Expression in the Adult Neural Stem Cell Niche *In Vivo* by Monocationic-based siRNA Delivery

Sylvie Remaud[1], Silvia Alejandra López-Juárez[1,2], Anne-Laure Bolcato-Bellemin[2], Patrick Neuberg[2], Fabrice Stock[2], Marie-Elise Bonnet[2], Rym Ghaddab[1], Marie Stéphanie Clerget-Froidevaux[1], Jacqueline Pierre-Simons[1], Patrick Erbacher[2], Barbara A Demeneix[1] and Ghislaine Morvan-Dubois[1]

RNA interference (RNAi) is a major tool for basic and applied investigations. However, obtaining RNAi data that have physiological significance requires investigation of regulations and therapeutic strategies in appropriate *in vivo* settings. To examine *in vivo* gene regulation and protein function in the adult neural stem cell (NSC) niche, we optimized a new non-viral vector for delivery of siRNA into the subventricular zone (SVZ). This brain region contains the neural stem and progenitor cells populations that express the stem cell marker, *SOX2*. Temporally and spatially controlled *Sox2* knockdown was achieved using the monocationic lipid vector, IC10. siRNA/IC10 complexes were stable over time and smaller (<40 nm) than jetSi complexes (≈400 nm). Immunocytochemistry showed that siRNA/IC10 complexes efficiently target both the progenitor and stem cell populations in the adult SVZ. Injection of the complexes into the lateral brain ventricle resulted in specific knockdown of *Sox2* in the SVZ. Furthermore, IC10-mediated transient *in vivo* knockdown of *Sox2*-modulated expression of several genes implicated in NSC maintenance. Taken together, these data show that IC10 cationic lipid formulation can efficiently vectorize siRNA in a specific area of the adult mouse brain, achieving spatially and temporally defined loss of function.

Molecular Therapy–Nucleic Acids (2013) **2**, e89; doi:10.1038/mtna.2013.8; published online 23 April 2013
Subject Category: siRNAs, shRNAs, and miRNAs and Nanoparticles

Introduction

Achieving the therapeutic potential of siRNA-based cell fate manipulation requires *in vivo* analysis of molecular signaling pathways implicated in the pathogenesis of the disease considered, often requiring specific targeting of a defined subset of cells so as to avoid off-target effects. The *in vivo* context determines cellular responses through multiple parameters ranging from physical constraints, such as cellular barriers, to paracrine regulations. Moreover, despite the difficulty of adapting siRNA approaches *in vivo*, optimization in the integrated context avoids certain disadvantages of *in vitro* analysis. The main drawbacks encountered when using cell lines are the altered biological responses due to the *in vitro* non-physiological environment, chromatin modifications, rearrangements derived from multiple platings, and amplifications.

These physiological, anatomical, and cellular concepts are particularly pertinent to the study of the neural stem cell (NSC) niche as it has a very complex three-dimensional architecture and mix of cell types. These different cell types include the NSCs themselves that undergo asymmetric division and differentiation into transit amplifying progenitor (TAP) cells and which then undergo further differentiation into migratory neuroblasts. Studying the postnatal interplay between genes that control division and differentiation in the niche *in vivo* is difficult. Loss of function studies in mutant mice often show severe embryonic effects that impair analysis of function in later development. To circumvent the early developmental effects of generalized loss of function, two approaches can be used in later development or in the mature animal: (i) conditional loss of function by genetic engineering or spatially and temporally defined RNA interference (RNAi) using vectorized siRNA or shRNA[1] or (ii) genetic engineering strategies including conditional knockout in specific adult cell populations. However, this latter technology implies the generation and maintenance of multiple transgenic mouse lines. As for RNAi approaches, different techniques have been tested *in vivo*, including electroporation, retroviral transduction, or shRNA vectorization, but each technique has specific drawbacks. Electroporation techniques and "gene guns" are useful in muscle and skin, but neural cells are more sensitive than muscles to physical damage induced by mechanical and electroporation transfection.[2] Moreover, using electroporation has two drawbacks, the limitation of transfection to cells close to the electrode and the lack of specificity in transfected cell types. Retroviral-based techniques provide efficient overexpression of cDNA or shRNA, especially in the brain (for review see ref. 3). However, besides their potential pathogenicity, viruses most often entail DNA integration in the genome with resulting off-target effects[4] (reviewed in ref. 5). Although non-viral alternatives are often less efficient, they are also less hazardous. Previously, we described how plasmid-based shRNA cassettes complexed with a cationic polymer, polyethylenimine could efficiently transfect NSC and progenitors of the newborn and adult mouse lateral ventricle.[6] We demonstrated that a CMV-H1-shTRa1 (inhibiting Thyroid Hormone Receptor alpha 1, *TRα1* expression) efficiently

The first two authors contributed equally to this work.
[1]Laboratoire d'Evolution des Régulations Endocriniennes, MNHN, Paris, France; [2]Polyplus-transfection, BIOPARC, Boulevard Sébastien Brant, Illkirch, France. Correspondence: Barbara A Demeneix, Laboratoire d'Evolution des Régulations Endocriniennes, MNHN, UMR CNRS 7221, 7 rue Cuvier 75231 Paris Cedex 05, France. E-mail: demeneix@mnhn.fr
Keywords: adult neural stem cells; *in vivo*; monocationic lipid vector; non-viral transfection; siRNA; *Sox2*
Received 13 November 2012; accepted 25 January 2013; advance online publication 23 April 2013. doi:10.1038/mtna.2013.8

downregulated expression of *CyclinD1*, an endogenous thyroid hormone target gene in mouse brain.

Like plasmid DNA, siRNAs are negatively charged and cannot cross the cell membrane by free diffusion.[7] Several strategies have been used to overcome this limitation. One strategy is to use nanoparticles (reviewed in ref. 8). Ideally, nanoparticle size should range from 10 to 1,000 nm, *i.e.,* small enough to enter cells but not undergo direct elimination by the organism. Nevertheless, particles larger than 200 nm are recognized by the reticulo-endothelial system machinery and undergo clearance. Thus, nanoparticles should be in the 10–200 nm range to be fully efficient. The most promising nanoparticles for therapeutic siRNA delivery are carbon nanotubes, which can facilitate siRNA entry into malignant cells.[9] However, the long-term effects of carbon nanoparticles are still to be determined in term of toxicity. In contrast, lipid-based delivery is well tolerated by the organism, showing no toxicity.[9,10] Several cationic lipid transfection reagents have been adapted to deliver siRNA *in vitro* and *in vivo* (for review see ref. 10). Previous results have shown that a formulation of polycationic lipospermine and neutral lipids (jetSI and dioleoylphosphatidylethanolamine (DOPE), respectively) increase delivery of siRNA *in vivo*.[6,11–13] When injected into the lateral ventricle, siRNA/(jetSI/DOPE) complexes transfect cells in the neurogenic regions of newborn mice brain. This method provides specific gene silencing in newborn mice brain with picomolar levels of siRNA.[11] However, jetSI/DOPE was less efficient for transfection of a neurogenic region of the adult brain, the subventricular zone (SVZ).[6] This limitation is particularly restrictive in the field of adult NSC research, where more understanding of the mechanisms controlling neurogenesis and differentiation are required to advance therapies for neurodegenerative diseases.

To overcome this limitation, a new type of vector, based on a monocationic lipid engineered with an imidazolium polar head was tested and optimized. This type of vector is exemplified by INTERFERin that *in vitro* testing has shown to be more efficient than the previous generations of polycationic lipid (lipospermine derivatives). siRNA transfected with INTERFERin provides >90% silencing efficiency at picomolar/nanomolar levels in a wide variety of cells, and particularly primary neurons.[14–16] The main advantages of monocationic lipids based on a imidazolium ring are the low cell toxicity and the efficient destabilization of the endosome facilitating siRNA release into the cytoplasm (for review see ref. 17).

In this study, the physicochemical properties of complexes prepared with either a polycationic lipid (jetSI) or a preparation using a monocationic lipid-based formulation designed for *in vivo* use, IC10, were compared. *In vivo* experiments were designed to assess whether IC10 could efficiently trigger transient *in vivo* downregulation of a key gene expressed in the adult mouse NSC niche. The target gene chosen was *Sox2*. SOX2 plays a central role in adult somatic stem cell biology by integrating the signals from different pathways.[18] The role of *Sox2* in NSC maintenance is well established and its expression needs to be downregulated to allow first brain maturation[19] during development and second, NSC commitment in the SVZ of adult mice.[20] This gene was thus chosen as suitable target to optimize siRNA delivery with cationic lipids so as to develop a versatile methodology that would facilitate analysis of factors controlling NSC biology in adult mammals.

The results show that IC10 is the first generation of lipid-based siRNA vectors to provide efficient, spatially and temporally defined knockdown in the adult mouse brain.

Results

The physicochemical properties of IC10 favor cell transfection *in vivo*

A prerequisite for siRNA delivery *in vivo* is that the siRNA is protected from degradation and clearance. Furthermore, siRNA/vector complexes should be stable in physiological fluids and yet be able to release their cargo within the cytoplasm of the target cell. This constraint means that formulation needs to balance complex stability outside the cell with dissociation of the complex within the cell. A major factor affecting the physicochemical properties of complexes (charge, size, and stability) is the osmolarity of solutions used for formulation. Preparing complexes in glucose solution (5%), avoiding salt-induced aggregation, has been shown to favor formation of small, nanometer sized, particles and improves transfection of nucleic acids into mouse brain with both cationic polymers,[21] and lipids.[6,11] All complexes were therefore prepared in glucose (5%). The physicochemical properties of siRNA/IC10 complexes thus formulated were determined before testing the *in vivo* transfection capacities. Given our experience with jetSI/DOPE, another polycationic lipid adapted for siRNA delivery, it was used as a reference point for physicochemical characterization.

First, the minimal amount of vector required to complex a fixed amount of siRNA stably was determined. Different N/P charge ratios were tested, where *N* is the number of positive charges from the cationic lipid and *P* the number of negative charges supplied by the siRNA. Complexes were analyzed by agarose gel electrophoresis. Non-complexed siRNA will freely enter the gel, whereas the higher molecular weight and size of formed complexes will delay migration and fully complexed siRNA will not migrate. Using JetSI/DOPE at a N/P ratio of 3 fully complexed the totality of siRNA (24 pmol) (**Figure 1a**, left panel). In contrast, the same amount of siRNA was fully complexed with IC10 at N/P ratio of 1.5 (**Figure 1a** right panel). This result shows that IC10 has a higher affinity for siRNA than jetSI/DOPE.

Degradation of siRNA by RNase activity is a major obstacle to siRNA delivery *in vivo*. The capacity of jetSI/DOPE and IC10 to protect siRNA from degradation was thus tested. In the presence of RNase (see Materials and Methods), both formulations protect siRNA against the degradation within 2 hours of incubation with RNases as compared with naked siRNA (**Figure 1b**).

As siRNA/(jetSI/DOPE) complexes formed at N/P 5.4 to 7.2 are most efficient in the newborn brain,[11] a N/P ratio of 6 was chosen for this study. For IC10, *in vitro* data showed that higher N/P ratios (from N/P of 8 at 10 nmol/l to N/P of 80 at 1 nmol/l) promoted efficient siRNA delivery and gene silencing. It is known that the ratio of lipid to

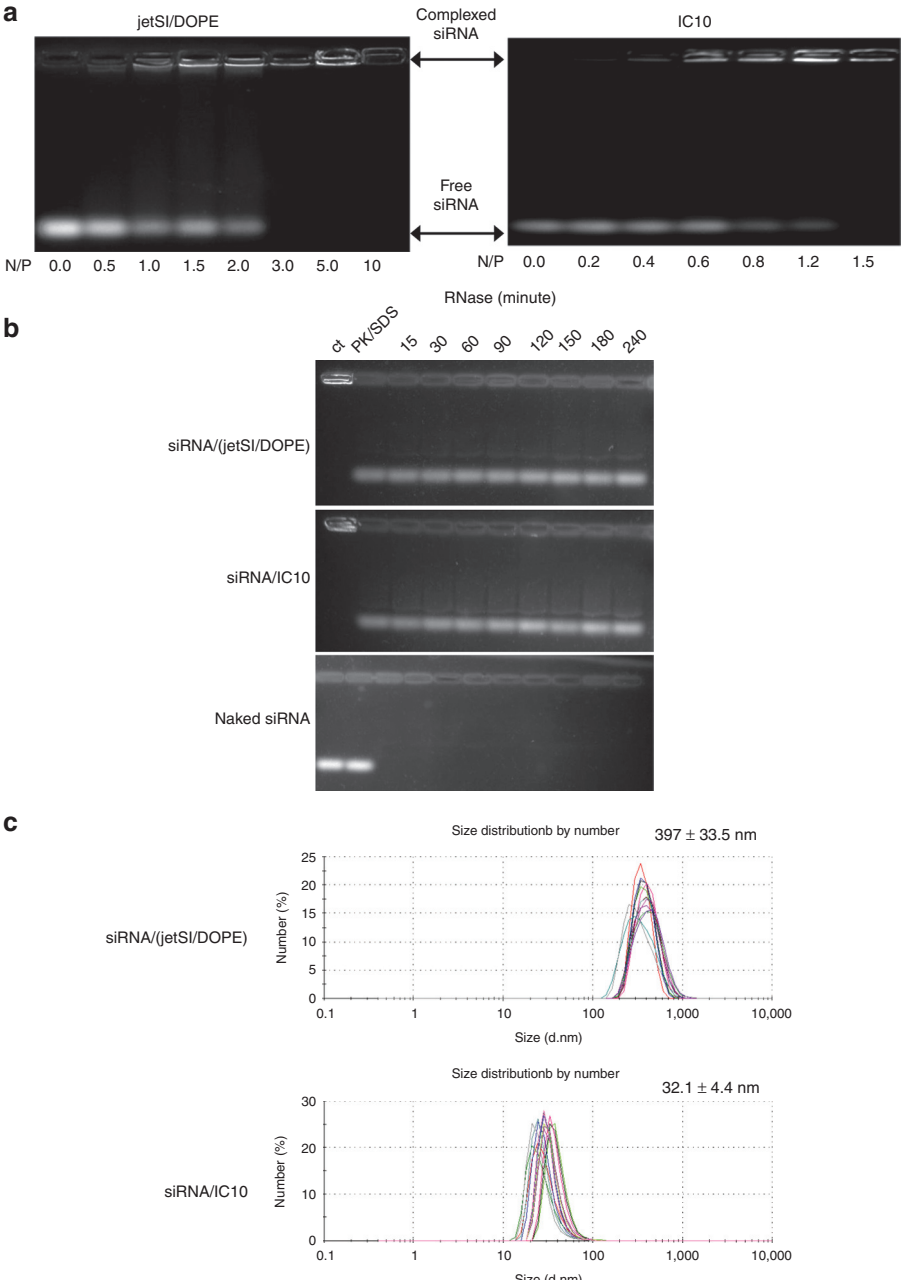

Figure 1 Polycationic versus monocationic lipids: Physicochemical characterization of siRNA/(jetSI/DOPE) and siRNA/IC10 complexes. Labeled siRNA (158.4 ng) were complexed with polycationic (jetSI/DOPE) or monocationic (IC10) lipids. (**a**) The minimal amount of lipid required to complex a fixed quantity of siRNA was determined by agarose gel electrophoresis. The stability of siRNA/(jetSI/DOPE) (left panel) and siRNA/IC10 (right panel) complexes presenting increasing lipid/siRNA (N/P) charge ratios was tested. siRNA complexed with jetSI/DOPE can be detected in wells corresponding to N/P = 0.5 to N/P = 10 and siRNA complexed with IC10 can be detected in the wells corresponding to N/P = 0.2 to N/P = 1.5 . Free siRNA migrates into the gel (for jetSI/DOPE N/P from 0 to 2 and for IC10 N/P from 0 to 1.2). (**b**) A RNase assay was performed on siRNA complexed with jetSI/DOPE at N/P = 1.8 (upper panel) and with IC10 at N/P = 15 (intermediate panel). A control experiment was performed with naked siRNA (lower panel). The integrity of siRNA was assessed at different time points, ranging from 15 to 240 minutes. Control lane contains siRNA complexes not treated with RNase. Note that the complexes remain in the well whereas naked siRNA migrates into the gel. siRNA is dissociated from the complexes in presence of SDS. (**c**) The size of particles formed by complexes siRNA/IC10 (at N/P 15) or siRNA/(jetSI/DOPE) (at N/P 6) was measured using a ZetaSizer Nano-ZS. Overplots of 15 measurement results and size mean ± SD of particles are shown. DOPE, dioleoylphosphatidylethanolamine.

siRNA is one of the key factors that strongly influences the shape, size, and behavior of lipoplexes.[22] The size of the complexes formulated for *in vivo* use, in 5% glucose solution, with IC10 at various N/P ratios and with jetSI/DOPE at N/P ratio of 6 was evaluated by dynamic light scattering. The size of siRNA/(jetSI/DOPE) complexes was 397.0 ± 33.5 nm (mean ± SEM, n = 15). However, complexes were one order of magnitude smaller with a mean size of

32.1 ± 4.4 nm (**Figure 1c**) when formed with IC10 at N/P 15. The zeta potentials of siRNA/IC10 and siRNA/(jetSi/DOPE) complexes were +62.1 ± 3.3 mV and +46.7 ± 7.8 mV, respectively. These very small and positively charged siRNA/IC10 complexes were found also to be stable within 4 hours of incubation with measured size variation <8%. For these reasons, we decided to continue our study with complexes formed at an N/P of 15.

siRNA/IC10 complexes efficiently transfect cells expressing NSC and progenitors markers

It has previously been shown that despite the high efficiency of jetSI/DOPE to deliver siRNA in the newborn brain,[11] it showed low efficiency in the adult brain. Hypothesizing that this lesser efficiency was due to limited diffusion in the mature extra-cellular matrix of the adult brain, the distribution of siRNA complexed with either jetSI/DOPE at N/P 6 or IC10 at N/P 15 was examined. The ability of each lipid-based formulation to deliver siRNA into the adult mouse brain was analyzed. To this end, complexes formed with fluorescently labeled siRNA (8 pmol) were introduced into one lateral ventricle of adult mice by stereotaxic injection (**Figure 2a**) as the lateral ventricles border the SVZ. The distribution of Alexa Fluor 594–labeled siRNA was studied by light microscopy analysis at 24 hours after injection on cryo-sections including the SVZ. Brains injected with siRNA/IC10 complexes (**Figure 2c**) showed many more cells containing labeled siRNA signal (in red) compared with brains injected with siRNA/(jetSI/DOPE) complexes (**Figure 2b**). Higher magnification of the dotted areas showed that in both cases, the signal included bright spots, consistent with local concentration of the labeled siRNA (**Figure 2** b',c'). In both cases, the presence of siRNA was found in the first cellular

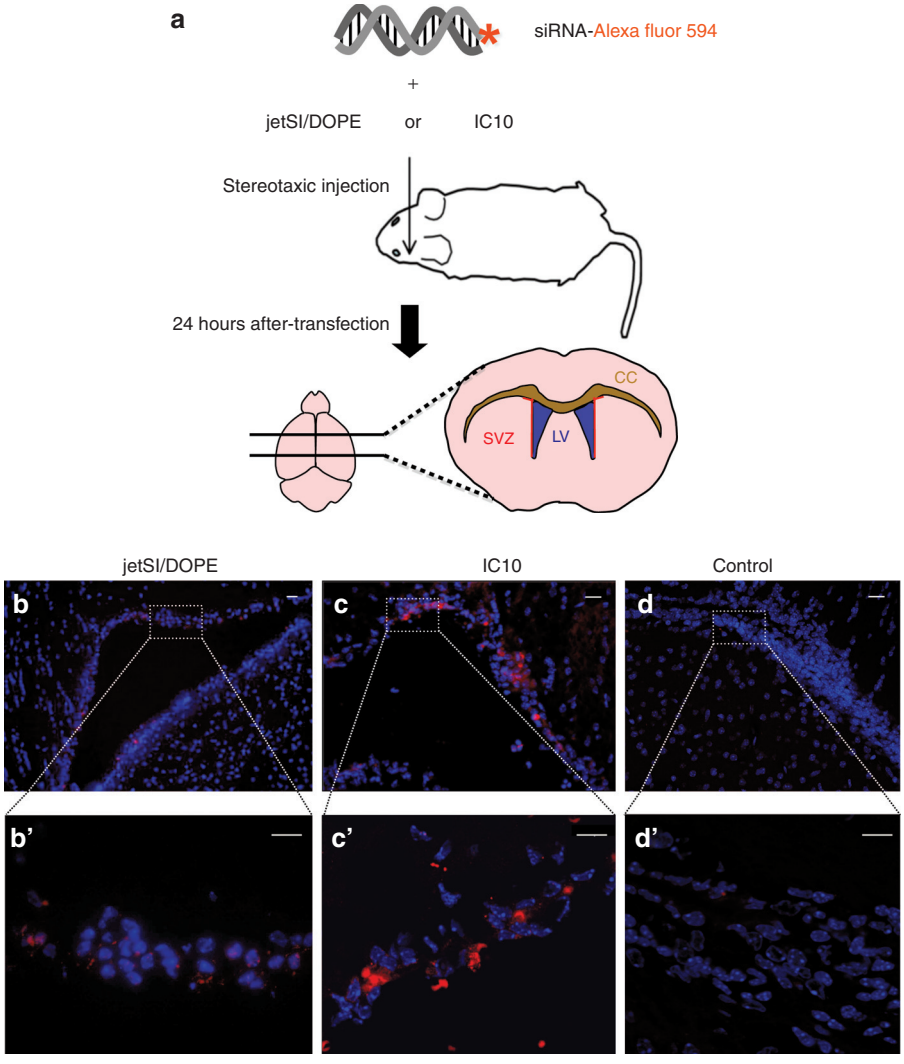

Figure 2 Distribution of vectorized siRNA with JetSI/DOPE and IC10 in the lateral ventricle of adult mice brain. (**a**) Schematic representation of procedures. Labeled siRNAs were complexed with jetSI/DOPE or IC10 and introduced into the lateral ventricle of adult mice brain by stereotaxic injection. siRNA distribution was analyzed in coronal brain sections. (**b**,**c**) In both cases, Alexa Fluor 594-siRNA (in red) was found around the whole SVZ area lining the lateral ventricle. Note that the siRNA signal was more intense and more widespread using complexes prepared with (**c**) IC10 rather than (**b**) jetSI/DOPE. High magnification of dotted area is shown in **b**' and **c**'. Scale bar: 20 µm. siRNA in red; nuclei stained with DAPI, in blue. (**d**). No signal above background is detected in control brains, injected with glucose. High magnification of dotted area is shown in **d**'. Scale bar: 20 µm. Nuclei stained with DAPI, in blue. DOPE, dioleoylphosphatidylethanolamine.

layers adjacent to the lateral ventricle, which corresponds to cells within the neurogenic niche.

The SVZ is a complex niche containing many cell types, including ependymal cells, blood vessel endothelial cells, NSCs, TAPs, and neuroblasts. Immunohistochemistry with a panel of antibodies directed against markers found in NSC and TAP (GFAP, NESTIN, and SOX2) (**Figure 3a**) was performed to identify the cell types targeted by siRNA/IC10 complexes. In most cases, the siRNA signal was observed in cells expressing either GFAP, NESTIN, or SOX2 (**Figure 3b–d** respectively). Different color merges are shown in **Figure 3** (b'–d') to clarify coexpression of markers in cells outlined by dots. The observed distribution of labeled siRNA indicates that IC10 vectorizes siRNA into cells expressing markers characteristic of NSC and TAP cells in the adult SVZ. Note that NESTIN and GFAP are cytoplasmic and SOX2 is nuclear, but the siRNA signal is always found in the cytoplasmic compartment.

IC10-vectorized siRNA efficiently downregulates expression of an endogenous target

Next, the efficiency of siRNA delivered with IC10 to inhibit expression of an endogenous target gene was investigated. As *Sox2* is expressed preferentially in NSC and TAPs that are transfected by IC10, the transcriptional modification induced by siRNA directed against *Sox2* mRNA was analyzed. siRNA targeting *Sox2* (siSox2) or control siRNA (siCtl) were complexed with IC10 at N/P ratio of 15. Complexes were introduced into the lateral ventricle of adult mice brains. SVZ were dissected 24 or 48 hours after injection and RNA was extracted from each sample. RT-qPCR was performed to quantify *Sox2* expression levels. In brains injected with siSox2, *Sox2* mRNA levels were significantly decreased ($P < 0.01$) by about 20% as compared with SVZ transfected with control siRNA (**Figure 4a**). At 48 hours, much more variability was seen in controls and siSox2 injected brains and the *sox2* levels were no longer significantly different. This result indicates that siRNA delivery by IC10 transiently silences the expression of an endogenous target gene in the NSC niche.

To determine if the transient knockdown in *Sox2* expression could trigger a decrease in SOX2 protein levels, the SOX2 content of the transfected SVZ was analyzed by western blotting (**Figure 4b**). To ensure that equivalent amounts of protein were blotted in each lane β-actin levels were determined. The amount of SOX2 detected in SVZ 48 hours after siSox2 injection was strongly decreased compared with SOX2 levels detected in SVZ of control group (injected with siCtl). This decrease in SOX2 level demonstrates that the transient knock-down observed 24 hours after siRNA injection was followed by a strong decrease in levels of the targeted protein. Immunohistochemistry using an antibody against SOX2 was performed on cryostat sections of SVZ from brain transfected with siSox2 or control siRNA (**Figure 4c**). Quantifying the SOX2 levels per DAPI-positive cell in the dorsal part of the SVZ showed a significantly decrease of SOX2 expression of about 25% ($P < 0.001$) following siSox2 transfection (**Figure 4d**).

Finally, we determined whether siSox2 vectorized with IC10 modulates downstream targets of SOX2 in a physiological manner. To this end, the mRNA levels of *Sox2* transcriptional targets were quantified using real time quantitative PCR. RNA

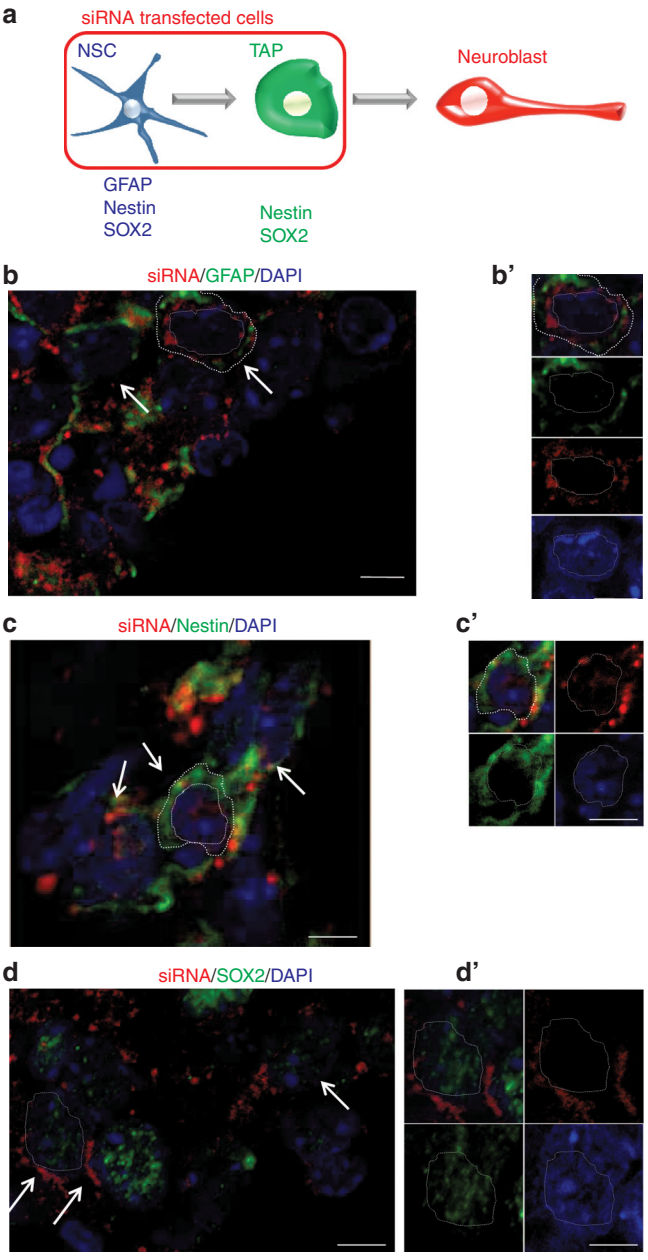

Figure 3 siRNA delivery by IC10 formulation targets neural stem cell (NSC) and transient amplificatory progenitor (TAP) populations of adult subventricular niche. (**a**) Schematic representation of NSC, TAP, and neuroblast markers. When injected into the adult mouse SVZ, IC10 is able to vectorize siRNA preferentially into NSC and TAPs. (**b**–**d**) Fluorescent immunohistochemistry against (**b**) GFAP (in green), (**c**) NESTIN (in green), or (**d**) SOX2 (in green). Arrows indicate cells containing siRNA (in red). These cells express NSC and/or TAP cellular markers. Different color merges are presented in **b'**–**d'** to clarify coexpression of markers in cells outlined by dots. Nuclei are labeled in blue with DAPI. Scale bar: 5 µm. SVZ, subventricular zone.

was extracted from SVZ of adult mice injected with siRNA directed against *Sox2* versus the control irrelevant siRNA. Both *Klf4* and *Nestin*, two known SOX2 targets were upregulated about threefold for *Klf4* (24 hours) and twofold for *Nestin* (48 hours) in adult SVZ injected with siSox2 compared with

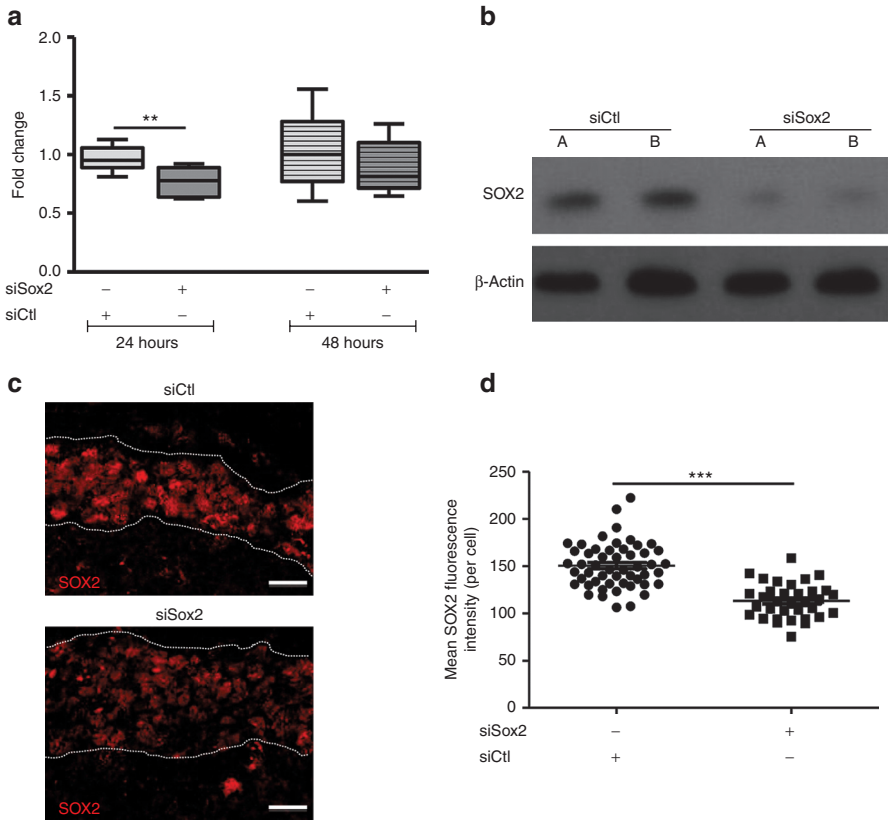

Figure 4 siRNA vectorized by IC10 into the adult SVZ efficiently decreases a specific endogenous target gene expression *in vivo*. siSox2 (158.4 ng or siPgl2 for control group) were introduced into the lateral ventricle of adult mice brain by stereotaxic injection. (**a**) qPCR quantification of *Sox2* mRNA was carried out on SVZ at 24 hours or 48 hours after injection. *Sox2* levels were normalized against *Gapdh* mRNA using the ΔΔCt method. Boxes represent the 5–95% around the median with whiskers for minimum and maximum values. The asterisks indicate that the difference between the pairs denoted are significant at the confidence levels $^{**}P < 0.01$ by exact non-parametric permutation test (Cytel Studio software). Each experiment was reproduced at least three times with $n > 3$ per group. (**b**) SOX2 expression levels were analyzed on SVZ (48 hours after injection) by western blot using anti-SOX2 and anti-b-TUBULIN antibodies. A decrease of SOX2 protein expression levels is observed in the SVZ transfected with siSox2 when compared with the control (siCtl). (**c**) Fluorescent immunohistochemistry against SOX2 (in red) was carried out on coronal sections of transfected brains (48 hours after injection). The SOX2 staining in the dorsal part of the SVZ is highlighted (dotted lines). Representative brains are shown. Scale bar: 20 µm. (**d**) Quantification of the amount of SOX2 per transfected cells after *Sox2* siRNA or control siRNA injection. The fluorescence was quantified by Fiji (see Materials and Methods) in each imaged nucleus of the SVZ. The number of SOX2 positive cells is significantly decreased following siSox2 injection. Statistical analysis was performed using non-parametric, exact permutation test for two independent samples (StatXact9, Cytel Studio software) $^{***}P < 0.001$. Means ± SEM are given. SVZ, subventricular zone.

control siRNA (**Figure 5**). Two other genes were found to be upregulated (*Shh* and *Cyclin D1*) but to a lower extent, and no significant effect was observed on *Mbp*. *Cyclin D1* expression was upregulated 24 hours after siSox2 injection, whereas *Shh* expression was unchanged 24 hours after injection but was upregulated 48 hours after siSox2 injection.

Discussion

Both basic and therapeutic studies ultimately require *in vivo* validation. In the case of the NSC niche, some aspects of the pathways controlling division and differentiation can be dissected out *in vitro*, but the endocrine, paracrine and the cell–cell interactions contribution are lost. To take these factors into account, the whole network of regulations needs to be analyzed in an *in vivo,* physiological context. Tools for invalidating gene expression *in vivo* exist and invalidation can be limited to the adult stem cell population by conditional mutagenesis, such as has been done in mutant mice.[23] However, this invalidation, even when used at later stages of development such as by using "conditional" knockouts, is long-term and results in a total loss of the targeted transcript, potentially inducing compensatory mechanisms. The interest of a moderate and transient alteration in gene expression, as seen with the methodology presented here, is that the whole network undergoes slight alteration and is not totally disrupted.

The data presented in this study show that duration of the knock down is limited, as *Sox2* mRNA level is no longer significantly decreased 48 hours after transfection. This is an advantage for transient study, as when using plasmids, even non-integrative plasmids, overexpression or downregulation of corresponding RNA and proteins can last several days. Although stable expression, such as obtained with integrative viruses, may be in many cases an advantage (e.g., for tumor targeting),[24] in other cases, it is not, as it is not possible to study

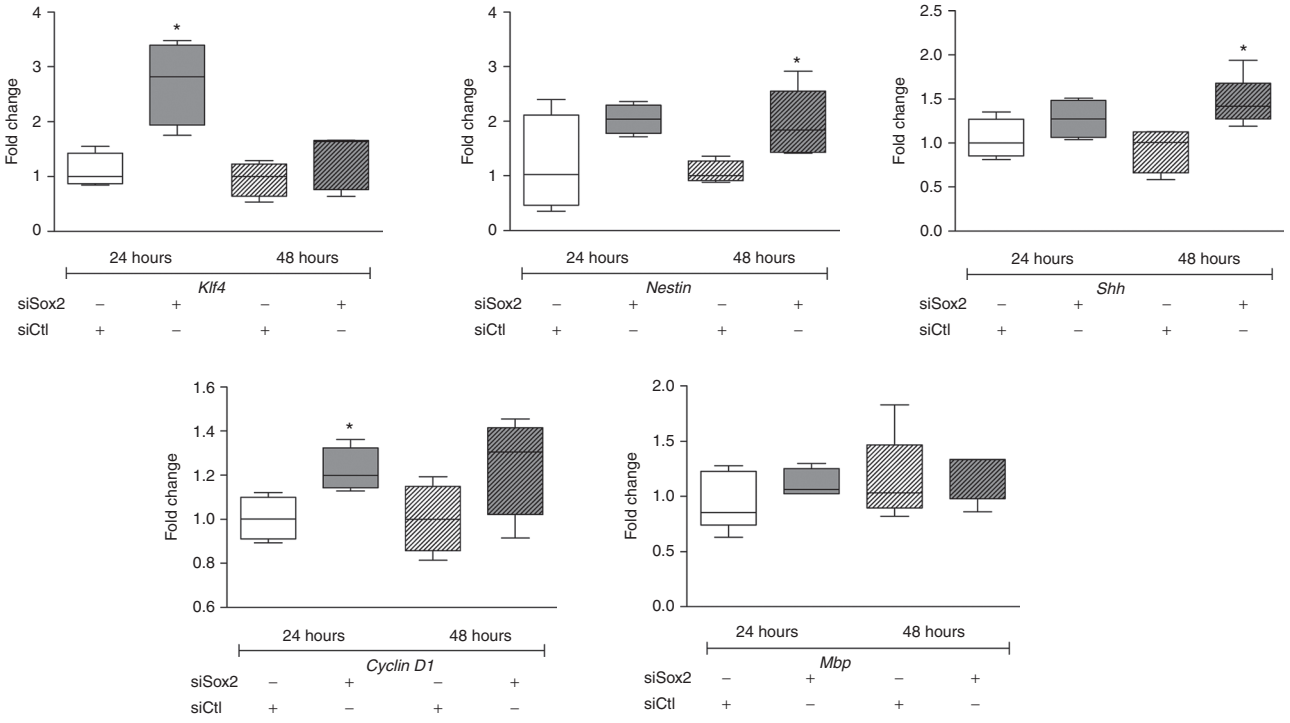

Figure 5 *In vivo* endogenous *Sox2* silencing by IC10-vectorized siRNA in adult mouse brain in modifies expression of markers of neural stem cell (NSC) self-renewal and differentiation. qPCR analysis of the effect of *Sox2* inhibition on mRNA encoding previously identified SOX2 direct targets. Note that expression of some stem cell markers such as *Nestin*, *Klf4*, *Shh*, and *Cyclin D1* are significantly upregulated, whereas expression of markers of neural differentiation (exemplified here by *Mbp*) is unchanged. Boxes and whiskers are as in Figure 4a. * indicates that *P* value was considered significant ($P < 0.05$).

how the population returns to equilibrium.[24] Finally, a transient knockdown better mimics the transcriptional regulations occurring in physiological conditions. Thus, transient siRNA-applied *in vivo* has the advantage of resembling physiological responses and regulations, an advantage that can be exploited.

siRNA-mediated gene knock-down is routinely used *in vitro*, where a number of transfection reagents can prove very efficient according to cell type studied. However, transposing this technique *in vivo* is often challenging, mainly because the *in vivo* environment is much more complex than culture media, the cells are by definition less accessible and many tissues are highly heterogeneous. What is more, as endogenous RNases are present in physiological fluids, including cerebro-spinal fluid, siRNA must be protected from endogenous RNase degradation *in vivo*. The results presented here demonstrate that IC10-based lipoplexes used at an N/P ratio of 15, and jetSI/DOPE lipoplexes used at N/P 6 are both resistant to RNase for up to 4 hours. The size of siRNA/IC10 complexes is an order of magnitude smaller than that of siRNA/(jetSI/DOPE), at N/P ratio of 15 and 6, respectively. The structure of cationic lipids can contribute to the smaller lipoplex size. IC10 contains a monocationic lipid based on a small polar head (methyl imidazolium salt) contrasting with the jetSI-based formulation that contains a polycationic spermine polar head. The smaller size, about 30 nm, of IC10 lipoplexes could contribute to better diffusion and to favor endocytosis, the most probable mechanism for cationic lipid-based complexes entry into the cell. The IC10 lipoplexes were found to be highly charged with a zeta potential >60 mV, a fact that explains the high stability of particles over time in solution as it will induce strong repulsion between particles. The small size as well as the stability of IC10 lipoplexes is controlled by the N/P ratio. IC10 complexes formed at a tenfold lower N/P ratio of 1.5 have a much larger size >100 nm and a lower zeta potential (about +15 mV) and are not stable in solution. Taken together, the different physicochemical properties analyzed show that siRNA/IC10 complexes formed at N/P ratio of 15 have several advantages, notably size and a high affinity to siRNA, in comparison with jetSI/DOPE complexes formed with optimal N/P ratio. These two principle features, explain why IC10 is the more efficient vector for siRNA in the adult mouse brain. In addition, the chemical composition of the cationic lipids may contribute to the observed difference in activity between the two lipoplex formulations. More investigations on the transfection mechanism are needed to clarify this point.

The need to study NSC division and differentiation in an *in vivo* context is underlined by the demonstration that NSCs in culture behave differently from endogenous NSC.[25] Thus, being able to apply siRNA *in vivo* provides a useful tool for studying basic NSC biology and for manipulating NSC fate in an integrated context. The distribution of fluorescently labeled siRNA injected into the lateral ventricle of adult mice by stereotaxic injection showed that siRNA/IC10 complexes delivered more siRNA into the first cellular layers compared with brains injected with siRNA/(jetSI/DOPE) complexes. The presence of siRNA was found in the cell layers adjacent to the lateral ventricle, which corresponds to cells of the neurogenic niche. In addition, immunocytochemistry confirmed that the cells targeted by siRNA/IC10 lipoplexes were part of the neurogenic

population, *i.e.,* NSCs and TAPs. This approach will be of specific use when studying NSC commitment and differentiation into specific lineages. Differentiation of NSC and TAPS into either neurons or oligodendrocytes is of particular importance in the field of neurodegenerative diseases where the physiology of a specific cell population is altered. Examples of therapeutic needs include dopaminergic neuron loss in Parkinson's disease or oligodendrocyte degeneration in multiple sclerosis. A recent study also revealed a potential role of aberrant adult NSC differentiation, correction of which could prove useful in Huntington's disease.[26] Such approaches using siRNA to modify the fate of endogenous NSC contrast with possible therapeutic stem cell–based approaches for neurodegenerative diseases employing embryonic stem cell grafts. Embryonic stem cell grafts have been demonstrated to improve neurodegenerative phenotypes in Parkinson's disease[27] and Huntington's disease (reviewed in ref. 28). However, the use of embryonic stem cell for *in vivo* therapy raises ethical and availability issues.

The question remains of whether transient and limited levels of knock-down seen with siRNA could exert useful therapeutic effects. In this set of experiments, we found that siRNA/IC10 complexes provided specific *Sox2* inhibition in NSC and TAP cells 24 hours after siRNA injection in adult brain. Although this inhibition of *Sox2* RNA only reached 20%, it was both highly significant ($P < 0.01$) and led to a major decrease in SOX2 protein levels in the SVZ. This fact indicates that the 20–25% reduction in the amount of *Sox2* mRNA has greater effects on SOX2 protein content in transfected cells. Furthermore, the expression of known SOX2 targets was significantly modified. This transcriptional regulation was most marked in the case of expression of *Klf4* and *Nestin* genes. Thus, this slight, but significant and physiological, decrease in *Sox2* expression is in turn sufficient to significantly modify adult SVZ homeostasis. Indeed, a similar decrease expression of *Sox2* in a mouse hypomorphic *Sox2* mutant (~25–30% relative to wild type) is sufficient to cause important brain defects: including decreased proliferation and the generation of newly neurons in the SVZ.[29] Moreover, we have recently shown that in mice lacking TRa (*TRa°/°*) the slight decrease of SOX2 levels (~22%) is associated with a reduction of neurogenesis in the adult SVZ.[20]

This study therefore demonstrates that *in vivo* transient downregulation of *Sox2* with IC10 is able to modify downstream key factors implicated in NSC and TAP physiology in the adult NSC niche. The result provides proof of concept that NSC can be manipulated *in vivo* in a temporal and spatially controlled manner.

Taking these results together shows that the IC10 vector bears numerous similarities to the "ideal vector" proposed by Kesharwani *et al.*[9] Such a vector would be small, of approximately viral size, have low toxicity, and display tissue specific distribution. Indeed, viruses, although more efficient than their non-viral counterparts, are difficult to constrain spatially. The localized sphere of action of IC10-vectorized siRNA is of particular interest in the SVZ, as cell fate depends on initial NSC localization.[30] The non-viral siRNA vectorization technology presented here can thus be of interest for fundamental research on NSC biology and for developing potential therapeutic leads.

Materials and methods

Animals and stereotaxic injections. All animal studies were conducted according to the principles and procedures described in Guidelines for Care and Use of Experimental Animal. Adult OF-1 male mice (8 weeks old, from Janvier, Le Genest St Isle, France) were anaesthetized with V-tranquile (2 mg/kg wt; Imalgen from Ceva Santé Animal, Libourne, France) followed by Ketamine (100 mg/kg wt; Imalgen from Merial, Lyon, France). A unilateral stereotaxic injection (5 µl) was performed into the right ventricle (0.2 mm posterior to bregma line, 1.1 mm lateral, and 2.2 mm deep from the pial surface). Analgesia treatment was performed using Meloxicam (Metacam from Boehringer Ingelheim, Ingelheim am Rhein, Germany).

siRNA complexes

Transfection agents: JetSI (dioctadecylamidoglycylspermine) 10 mmol/l was used with DOPE 20 mmol/l at a 1:2 molar ratio, as described in Hassani *et al.*[11] If not otherwise stated, JetSI and DOPE were used at the optimal N/P charge ratio of 5.4–7.2 previously determined.[11] IC10 is a monocationic lipid formulation based on a methyl-3H-imidazolium polar head (WO/2008004058). This lipid, 1-methyl-3-(1-octadecyl-nonadecyl)-3H-imidazol-1-ium chloride, is formulated into cationic liposome in presence of DOPE at molar ratio of 10/15 mmol/l in 20% ethanol in water. IC10 was used at N/P 15. JetSI and IC10 were supplied by Polyplus-Transfection (Illkirch, France). DOPE was from Sigma (St Louis, MO).

siRNA: All siRNA were obtained from Qiagen (Courtaboeuf, France). The different sequences used in this work are the follow:

1. Labeled siRNA, all stars negative control siRNA-Alexa Fluor 594.
2. SiCtl, siRNA against pGL2Luc (Target sequence: CGTACGCGGAATACTTCGATT).
3. siSox2. Four different sequences were used against *Sox2* at an equimolar ratio:
   Mm_Sox2_3, Target sequence 5′-CAGGTTGATATCGTT GGTAAT-3′
   Mm_Sox2_4, Target sequence 5′-AAGGAGCACCC GGATTATAAA-3′
   Mm_Sox2_5, Target sequence 5′-CAGCTCGCAGACC TACATGAA-3′
   Mm_Sox2_6, Target sequence 5′-TAGGACCGTTACAAA CAAGGA-3′

Formulation of complexes siRNA/(jetSI/DOPE): All complexes were prepared under RNase free conditions. The formulations of siRNA/(jetSI/DOPE) were prepared as described in ref 11. Briefly, for a siRNA/(jetSI/DOPE) complex containing 24 pmol of siRNA at N/P 6 in 5 µl of solution, two separate solutions were prepared. Solution A, containing siRNA (at 9.4 µmol/l) were diluted in 25 µl of glucose solution (5%). Solution B containing 3.5 µl of jetSI/DOPE (5 mmol/l/10 mmol/l) diluted in 25 µl of glucose solution (5%). Solution A was added to solution B. Immediately after mixing, the solutions were continuously vortexed for 30 seconds. Complexes were incubated at room temperature for 10 minutes before stereotaxic injection. To detect background fluorescence in the immunolabeling experiments, control brains were injected with glucose solution (5%).

Formulation of complexes siRNA-IC10: A siRNA/IC10 complex containing 24 pmol of siRNA at N/P 15 in 5 µl of solution was prepared as follows: To prepare 50 µl of final solution, siRNA (at 4.8 µmol/l) were diluted in glucose solution (5%). The volume of IC10 necessary to complex siRNA at N/P 15 (15 µl) was added directly into the siRNA mix, then vortexed continuously for 30 seconds. Complexes were incubated at room temperature for 10 minutes before stereotaxic injection.

Determination of the minimal N/P ratio to complex siRNA: The ability to complex 24 pmol of siRNA at different N/P ratios was tested for both monocationic and polycationic formulation by gel electrophoresis assay. For jetSI/DOPE formulation, the N/P ratio ranges from 0 to 10. For IC10 formulation, the N/P ratio ranges from 0 to 1.5. Complex formation was analyzed by agarose gel electrophoresis (1.2%), stained with ethidium bromide and visualized under UV.

Protection from RNase-mediated degradation: IC10 complexes were prepared at N/P ratio of 15 and siRNA/(jetSI/DOPE) complexes at N/P ratio of 6. Resistance of complexes to RNase-mediated degradation was determined by electrophoresis assay and ethidium bromide staining.[31] Complexes, containing 250 ng of siRNA and prepared in glucose solution (5%), were incubated for times ranging from 5 minutes to 4 hours at 37 °C, in the presence of 1 µg of RNase V1 (Ambion, Life Technologies SAS, Saint Aubin, France). After incubation, RNase was inactivated by proteinase K (0.35 µg) and complexes dissociated in presence of SDS (0.65%) at 37 °C for 30 minutes and then analyzed by agarose gel electrophoresis (1.2%). After gel electrophoresis, gel was stained with ethidium bromide and visualized under UV.

Particle size and zeta potential measurements: IC10 complexes were prepared at N/P ratio of 15 and siRNA/(jetSI/DOPE) complexes were prepared at N/P ratio of 6. Four hundred microliters of each solution were prepared at room temperature. Particle size was determined by dynamic light scattering using a ZetaSizer Nano-ZS (Malvern Instrument, Orsay, France) with the following specifications: sampling time, 60 seconds; 15 measurements per sample; medium viscosity, 1.014 cP; refractive index medium, 1.34; refractive index particle, 1.45; temperature, 20 °C. Zeta potential was determined with the following specifications: dielectric constant, 78.5.

Immunohistochemistry techniques

Brain perfusion: Mice were deeply anesthetized with Pentobarbital (130 mg/kg from Sanofi, Libourne, France) then sequentially perfused (3 ml/minutes) with saline solution (0.9%). Brains were dissected and fixed in paraformaldehyde (2%) in phosphate-buffered saline (0.1 mol/l, pH 7.4) at 4 °C overnight, and cryoprotected in sucrose (30%).

Cryosection: Cryoprotected brains were embedded in OCT, frozen and stored at –80 °C. 30 µm cryostat coronal brain sections were made, then the slices were immersed in TRIS-buffered saline (TBS) briefly. Post-fixation was done in paraformaldehyde 2% during 5 minutes, then the floating sections were rinsed in TBS before proceeding with immunostaining.

Immunostaining: After 1 hour blockage in phosphate-buffered saline + Normal Donkey Serum (Sigma), floating sections were incubated overnight at 4 °C with one of the following primary antibodies: mouse monoclonal anti-NESTIN (Abcam, Paris, France; ab6142, 1:1,000), rabbit polyclonal anti-GFAP (Dako, Carpinteria, CA; Z0334, 1:500), or rabbit anti-SOX2 (Chemicon, Millipore SAS, Molsheim, France; 1:200). Samples were washed twice in phosphate-buffered saline and incubated with corresponding secondary antibodies: donkey antimouse IgG Alexa Fluor 488 (Molecular Probes, Life Technologies SAS, Saint Aubin, France; 1:500), or donkey antirabbit IgG Alexa Fluor 488 nm (Molecular Probes; 1:500) for 2 hours at room temperature. Sections were mounted in Super-Frost Ultra Plus slides (Menzel-Glaser, Braunschweig, Germany) in Prolong Gold Antifade (containing the nuclear marker, DAPI (Invitrogen, Carlsbad, CA; P-36931). Fluorescence microscopy was performed on a Zeiss Axiovert 200 inverted microscope and ApoTome system (Carl Zeiss, Thomwood, NY) and confocal imaging was performed on a LEICA SP5.

Quantitative real time PCR. SVZs of adult brains were dissected under a dissecting microscope in RNase free conditions. Tissue was snap-frozen in liquid nitrogen and stored at –80 °C until processing. Total RNA was extracted using RNAble (Eurobio, Les Ulis, France) and purified on RNeasy minelute cleanup column (Qiagen). Concentration of total RNA was measured on a Nanodrop and RNAs stored at –80 °C. To quantify specific mRNAs expression, 1 µg of total RNA was reverse-transcribed using High capacity cDNA Reverse Transcription kit (Applied Biosystems, Courtaboeuf, France). Control reactions without reverse transcriptase were done in parallel. Primers from Taqman gene expression assays were used for the mRNA detection: *Sox2 (*Mm03053810_s1), *CyclinD1* (Mm00432360_g1), *Nestin* (Mm01223404_g1), *Klf4* (Mm00516104_m1), *Sonic hedgehog* (Mm00436528_m1), and *Myelin basic protein* (Mm01266402_m1). The *Gapdh* (Mm99999915_g1) was used as an endogenous control gene for normalization. The relative differences of expression between the control and treated groups were quantified using the $2^{-\Delta\Delta CT}$ method.

Immunoblot analysis. Western blot analysis was done on SVZ protein extract from brains transfected with siRNA/IC10 complexes. Briefly, the SVZs of two distinct mice were collected for each group under a dissecting microscope. The whole experiment was repeated twice. Tissues were lysed mechanically and proteins were extracted in RIPA buffer (150 mmol/l NaCl, 1% Triton X-100, 0.5% sodium deoxycholate, 0.1% SDS, and 50 mmol/l Tris pH 8) according to the manufacturer instructions. Protein content was determined by Qbit assays (Invitrogen). Total cell lysates (30 µg) were fractionated by SDS-PAGE 4–20% (Pierce, Fisher Scientific, Illkirch, France) and transferred to nitrocellulose membranes (Biorad, Hercules, CA). Membranes were blocked with 5% nonfat milk in TBS (10 mmol/l Tris–HCl, pH 7.5, 150 mmol/l NaCl), followed by overnight incubation at 4 °C with the indicated antibody diluted in TBS with 0.05% Tween-20 (TBS-T). After three washes with TBS-T, membranes were incubated with the appropriate secondary antibody coupled to horseradish peroxidase, and immunocomplexes visualized by enhanced chemiluminescence according to manufacturer's instructions (Promega, Madison, WI). Primary antibodies for western

blotting included rabbit polyclonal anti-SOX2 (1:200; Millipore, Billerica, MA), rabbit polyclonal anti-βACTIN (1:5,000; Thermo Fisher, Villebon sur Yvette, France). Secondary antibody was HRP conjugated anti rabbit from Sigma. Imaging was performed on BioRad Imager.

Statistical analysis. Cytel Studio software was used for statistical analysis. Results are expressed as the mean ± SEM from an appropriate number of experiments as indicated in figure legends. Statistical differences were analyzed with the Mann–Whitney *U* test for non-parametric values to compare control and treated groups. $P < 0.05$ was considered significant ($^{*}P < 0.05$; $^{**}P < 0.01$; $^{***}P < 0.001$).

Acknowledgments. We thank the IJM imaging platform and G Levi for insightful comments. The excellent animal care provided by Stéphane Sosinsky, Philippe Durand, and Fabien Uridat is gratefully acknowledged. This work was supported by the Centre National de la Recherche Scientifique (CNRS), the Museum National d'Histoire Naturelle (MNHN), the Association Française contre les Myopathies (AFM) "[grant number MNM1 2012–14685]," European Union contracts "Crescendo" "[grant number LSHM-CT-2005–018652]," Switchbox "[grant number FP7-Health-2010 n° 259772]," and the French ANR "Thrast" "[grant number 11BSV2 019 02]." A.L.-J. received a PhD grant from the Association national de la Recherche et technologie (ANRT) and Polyplus-transfection S.A. under CIFRE convention "[grant number 251/2007]." Funding for open access charge: AFM "[grant number MNM1 2012–14685]." The authors declare no conflict of interest.

1. Brummelkamp, TR, Bernards, R and Agami, R (2002). A system for stable expression of short interfering RNAs in mammalian cells. *Science* **296**: 550–553.
2. Murakami, T and Sunada, Y (2011). Plasmid DNA gene therapy by electroporation: principles and recent advances. *Curr Gene Ther* **11**: 447–456.
3. Sliva, K and Schnierle, BS (2010). Selective gene silencing by viral delivery of short hairpin RNA. *Virol J* **7**: 248.
4. Biasco, L, Ambrosi, A, Pellin, D, Bartholomae, C, Brigida, I, Roncarolo, MG *et al.* (2011). Integration profile of retroviral vector in gene therapy treated patients is cell-specific according to gene expression and chromatin conformation of target cell. *EMBO Mol Med* **3**: 89–101.
5. Biasco, L, Baricordi, C and Aiuti, A (2012). Retroviral integrations in gene therapy trials. *Mol Ther* **20**: 709–716.
6. Hassani, Z, François, JC, Alfama, G, Dubois, GM, Paris, M, Giovannangeli, C *et al.* (2007). A hybrid CMV-H1 construct improves efficiency of PEI-delivered shRNA in the mouse brain. *Nucleic Acids Res* **35**: e65.
7. Lu, JJ, Langer, R and Chen, J (2009). A novel mechanism is involved in cationic lipid-mediated functional siRNA delivery. *Mol Pharm* **6**: 763–771.
8. Snead, NM and Rossi, JJ (2012). RNA interference trigger variants: getting the most out of RNA for RNA interference-based therapeutics. *Nucleic Acid Ther* **22**: 139–146.
9. Kesharwani, P, Gajbhiye, V and Jain, NK (2012). A review of nanocarriers for the delivery of small interfering RNA. *Biomaterials* **33**: 7138–7150.
10. de Fougerolles, AR (2008). Delivery vehicles for small interfering RNA in vivo. *Hum Gene Ther* **19**: 125–132.
11. Hassani, Z, Lemkine, GF, Erbacher, P, Palmier, K, Alfama, G, Giovannangeli, C *et al.* (2005). Lipid-mediated siRNA delivery down-regulates exogenous gene expression in the mouse brain at picomolar levels. *J Gene Med* **7**: 198–207.
12. Decherf, S, Seugnet, I, Kouidhi, S, Lopez-Juarez, A, Clerget-Froidevaux, MS and Demeneix, BA (2010). Thyroid hormone exerts negative feedback on hypothalamic type 4 melanocortin receptor expression. *Proc Natl Acad Sci USA* **107**: 4471–4476.
13. Niizuma, K, Endo, H, Nito, C, Myer, DJ, Kim, GS and Chan, PH (2008). The PIDDosome mediates delayed death of hippocampal CA1 neurons after transient global cerebral ischemia in rats. *Proc Natl Acad Sci USA* **105**: 16368–16373.
14. Araújo, IM, Carreira, BP, Pereira, T, Santos, PF, Soulet, D, Inácio, A *et al.* (2007). Changes in calcium dynamics following the reversal of the sodium-calcium exchanger have a key role in AMPA receptor-mediated neurodegeneration via calpain activation in hippocampal neurons. *Cell Death Differ* **14**: 1635–1646.
15. Briane, D, Slimani, H, Tagounits, A, Naejus, R, Haddad, O, Coudert, R *et al.* (2012). Inhibition of VEGF expression in A431 and MDA-MB-231 tumour cells by cationic lipid-mediated siRNA delivery. *J Drug Target* **20**: 347–354.
16. Bordji, K, Becerril-Ortega, J, Nicole, O and Buisson, A (2010). Activation of extrasynaptic, but not synaptic, NMDA receptors modifies amyloid precursor protein expression pattern and increases amyloid-ß production. *J Neurosci* **30**: 15927–15942.
17. Midoux, P, Pichon, C, Yaouanc, JJ and Jaffrès, PA (2009). Chemical vectors for gene delivery: a current review on polymers, peptides and lipids containing histidine or imidazole as nucleic acids carriers. *Br J Pharmacol* **157**: 166–178.
18. Pevny, LH and Nicolis, SK (2010). Sox2 roles in neural stem cells. *Int J Biochem Cell Biol* **42**: 421–424.
19. Mariani, J, Favaro, R, Lancini, C, Vaccari, G, Ferri, AL, Bertolini, J *et al.* (2012). Emx2 is a dose-dependent negative regulator of Sox2 telencephalic enhancers. *Nucleic Acids Res* **40**: 6461–6476.
20. López-Juárez, A, Remaud, S, Hassani, Z, Jolivet, P, Pierre Simons, J, Sontag, T *et al.* (2012). Thyroid hormone signaling acts as a neurogenic switch by repressing Sox2 in the adult neural stem cell niche. *Cell Stem Cell* **10**: 531–543.
21. Goula, D, Benoist, C, Mantero, S, Merlo, G, Levi, G and Demeneix, BA (1998). Polyethylenimine-based intravenous delivery of transgenes to mouse lung. *Gene Ther* **5**: 1291–1295.
22. Schiffelers, RM, Mixson, AJ, Ansari, AM, Fens, MH, Tang, Q, Zhou, Q *et al.* (2005). Transporting silence: design of carriers for siRNA to angiogenic endothelium. *J Control Release* **109**: 5–14.
23. Takeda, H, Koso, H, Tessarollo, L, Copeland, NG and Jenkins, NA (2013). Musashi1-CreER(T2): a new cre line for conditional mutagenesis in neural stem cells. *Genesis* **51**: 128–134.
24. Schaser, T, Wrede, C, Duerner, L, Sliva, K, Cichutek, K, Schnierle, B *et al.* (2011). RNAi-mediated gene silencing in tumour tissue using replication-competent retroviral vectors. *Gene Ther* **18**: 953–960.
25. Pastrana, E, Cheng, LC and Doetsch, F (2009). Simultaneous prospective purification of adult subventricular zone neural stem cells and their progeny. *Proc Natl Acad Sci USA* **106**: 6387–6392.
26. Conforti, P, Camnasio, S, Mutti, C, Valenza, M, Thompson, M, Fossale, E *et al.* (2013). Lack of huntingtin promotes neural stem cells differentiation into glial cells while neurons expressing huntingtin with expanded polyglutamine tracts undergo cell death. *Neurobiol Dis* **50**: 160–170.
27. Ganat, YM, Calder, EL, Kriks, S, Nelander, J, Tu, EY, Jia, F *et al.* (2012). Identification of embryonic stem cell-derived midbrain dopaminergic neurons for engraftment. *J Clin Invest* **122**: 2928–2939.
28. Maucksch, C, Vazey, EM, Gordon, RJ and Connor, B (2013). Stem cell-based therapy for Huntington's disease. *J Cell Biochem* **114**: 754–763.
29. Ferri, AL, Cavallaro, M, Braida, D, Di Cristofano, A, Canta, A, Vezzani, A *et al.* (2004). Sox2 deficiency causes neurodegeneration and impaired neurogenesis in the adult mouse brain. *Development* **131**: 3805–3819.
30. Lledo, PM, Merkle, FT and Alvarez-Buylla, A (2008). Origin and function of olfactory bulb interneuron diversity. *Trends Neurosci* **31**: 392–400.
31. Cardoso, AL, Simões, S, de Almeida, LP, Pelisek, J, Culmsee, C, Wagner, E *et al.* (2007). siRNA delivery by a transferrin-associated lipid-based vector: a non-viral strategy to mediate gene silencing. *J Gene Med* **9**: 170–183.